OPEN

Oncogene (2014) **33,** 4407–4417

www.nature.com/onc

ORIGINAL ARTICLE

Wig-1 regulates cell cycle arrest and cell death through the p53 targets FAS and 14-3-3σ

C Bersani, L-D Xu, A Vilborg[1], W-O Lui and KG Wiman

Wig-1, also known as ZMAT3, is a p53 target gene that encodes an RNA-binding zinc-finger protein involved in the regulation of mRNA stability through binding to AU-rich elements (AREs). We have used microarray analysis to identify novel Wig-1 target mRNAs. We identified 2447 transcripts with >fourfold differential expression between Wig-1 and control small interfering (si)RNA-treated HCT116 cells. Several p53 target genes were among the deregulated transcripts. We found that Wig-1 regulates FAS and 14-3-3σ mRNA independently of p53. We show that Wig-1 binds to FAS mRNA 3′-UTR and decreases its stability through an ARE in the 3′-UTR. Depletion of Wig-1 was associated with increased cell death and reduced cell cycle arrest upon DNA damage. Our results suggest a role of Wig-1 as a survival factor that directs the p53 stress response toward cell cycle arrest rather than apoptosis through the regulation of FAS and 14-3-3σ mRNA levels.

Oncogene (2014) **33,** 4407–4417; doi:10.1038/onc.2013.594; published online 27 January 2014

Keywords: Wig-1; p53; FAS; 14-3-3σ; AU-rich element; AU-rich element-binding proteins

INTRODUCTION

The tumor suppressor p53 is a transcription factor that is activated in response to cellular stress, including DNA damage and oncogene activation. p53 regulates a wide range of cellular processes, mainly through transcriptional activation of downstream target genes.[1] p53 induces cell cycle arrest mainly through p21[2] and 14-3-3σ,[3] and induces apoptosis through target genes such as FAS,[4] PUMA[5] and NOXA.[6] The molecular mechanisms underlying the cell's decision to enter growth arrest or to undergo apoptosis in response to p53 activation are only partly understood. p53 function is affected by cell type, genetic background, microenvironment and the nature of the stress that the cell is exposed to.[1] It was proposed that low or moderate p53 induction can lead to cell cycle arrest, whereas higher levels of p53 can trigger apoptosis.[7] p53 has different binding affinity to promoters of proarrest target genes and of proapoptotic targets, and this affinity might be regulated by post-translational modifications of p53.[8]

Wig-1 (ZMAT3) is a p53 target gene involved in the regulation of mRNA stability.[9] The Wig-1 protein contains three highly conserved C2H2-type zinc-fingers[10,11] and binds double-stranded RNA with high affinity through the first and second zinc-finger.[12,13] Wig-1 is an AU-rich element (ARE)-binding protein (ARE-BP) and positively regulates p53 and N-Myc mRNAs[14,15] through direct binding to AREs in the 3′-UTRs of these mRNAs. AREs are present in 10–15% of all transcripts, and they regulate mRNA turnover and translation. ARE-BPs exert post-transcriptional control through binding to AREs and regulate gene expression through mRNA stability and/or translation efficiency.[16] An ARE-BP can destabilize a target mRNA by recruiting enzymes involved in both 5′→3′ and 3′→5′ mRNA decay[17] or stabilize a target mRNA by preventing the actions of such enzymes.[18] In addition, ARE-BPs can regulate almost all aspects of RNA metabolism including alternative splicing, nucleocytoplasmic export, cytoplasmic localization and translational efficiency.[17,19,20] The importance of ARE-mediated regulation has been studied for several targets,[14,21–24] whereas the functionality of the ARE in other mRNAs, such as FAS, remains to be experimentally demonstrated. Most ARE-BPs have multiple mRNA targets, suggesting that Wig-1 could bind to and regulate other ARE-containing mRNAs apart from p53 and N-Myc.

Here we present a global approach to study Wig-1 target mRNAs. We identified 2447 transcripts that were affected by Wig-1 knockdown. We found that FAS and14-3-3σ mRNAs are regulated by Wig-1 independently of p53, and that the absence of Wig-1 is associated with increased cell death and reduced cell cycle arrest in response to DNA damage. We propose that Wig-1 is a regulator of the cellular stress response and can act as a prosurvival factor downstream of p53 upon cellular stress.

RESULTS

Identification of putative Wig-1 target genes by gene expression profiling

To identify putative Wig-1 targets, we performed global gene expression profiling on HCT116 cells transfected with siRNA against Wig-1 (siW1) or control siRNA. We chose siW1 because it was the most effective siRNA for Wig-1 knockdown.[15] After normalization and filtration of data, we obtained 2447 transcripts whose expression showed a >fourfold difference in at least two out of the three replicates (Supplementary Table 1). Using the PANTHER software to classify these differentially expressed genes into pathways, biological processes and molecular function, we found that the most significantly deregulated pathways upon Wig-1 silencing included Alzheimer's and Huntington's diseases, the p53 pathway, the FAS signaling pathway and apoptosis. Metabolic

Cancer Center Karolinska (CCK), Department of Oncology-Pathology, Karolinska Institute, Stockholm, Sweden. Correspondence: Professor KG Wiman, Cancer Center Karolinska (CCK), Department of Oncology-Pathology, Karolinska Institute, SE-171 76 Stockholm, Sweden.
E-mail: Klas.Wiman@ki.se
[1]Current address: Department of Molecular Biophysics and Biochemistry, BCMM 133, Yale University, New Haven, CT 06510, USA
Received 6 May 2013; revised 31 October 2013; accepted 16 December 2013; published online 27 January 2014

processes and cell cycle were the most significantly affected biological processes, and molecular functions such as catalysis, binding and transport showed substantial deregulation after Wig-1 knockdown (Table 1).

To validate the microarray findings, eight targets were selected based on the extent of changes in expression in the microarray analysis, the presence of AREs in their 3′-UTR and known involvement in the most affected pathways (Figure 1a). We analyzed the protein levels of the selected eight targets in HCT116 cells transfected with control siRNA or two different siRNAs against Wig-1 (siW1, siW2), using the same conditions as for the microarray experiments. We were able to confirm changes of FAS, WNT1, AKT3, APP, 14-3-3σ and PPP2CB at the protein level (Figures 1b–d and f). The changes in protein levels for FZD8 and CDC42 were inconsistent with the microarray data (Supplementary Figure 1).

Wig-1 knockdown causes upregulation of FAS and downregulation of 14-3-3σ

Given that Wig-1 is a p53 target gene and the p53 pathway was one of the most affected pathways after Wig-1 knockdown (Table 1 and Supplementary Table 2), we chose to study the effect of Wig-1 expression on the p53 pathway in further detail. We investigated the Wig-1 effect on the proapoptotic FAS gene and the cell cycle arrest 14-3-3σ gene as they showed the most pronounced changes in expression after Wig-1 knockdown. FAS, but not 14-3-3σ, contains an ARE in its 3′-UTR.

Wig-1 is upregulated after stress in a p53-dependent manner[10] (Figure 1e), suggesting that Wig-1 has a stress-related function. We therefore induced DNA damage with cisplatin in HCT116 cells. Silencing of Wig-1 led to a decrease of 14-3-3σ and an increase of FAS protein levels also after cisplatin treatment (Figures 1f and g). To further determine whether this effect of Wig-1 is p53-dependent, we assessed the expression of both targets by qRT–PCR in HCT116 $p53^{+/+}$ and $p53^{-/-}$ cells with or without cisplatin-induced stress. We found a modest decrease of 14-3-3σ and a significant increase of FAS mRNA levels in both p53 wild-type and null HCT116 cells with and without cisplatin treatment upon Wig-1 knockdown (Figure 1h). This demonstrates that Wig-1 regulates FAS and 14-3-3σ independently of p53. Both HCT116 $p53^{+/+}$ and $p53^{-/-}$ cells express relatively high basal levels of Wig-1.

Table 1. Functional annotation of Wig-1 target genes using PANTHER

	P-*value*[a]
Pathways	
Alzheimer's disease-presenilin pathway	1.43E − 03
Huntington's disease	2.54E − 03
p53 pathway	2.64E − 03
Formyltetrahydroformate biosynthesis	2.02E − 02
FAS signaling pathway	2.09E − 02
Cadherin signaling pathway	2.20E − 02
Wnt signaling pathway	2.37E − 02
S adenosyl methionine biosynthesis	3.22E − 02
Purine metabolism	3.94E − 02
Apoptosis signaling pathway	4.24E − 02
Biological process	
Metabolic process	3.50E − 15
Primary metabolic process	1.47E − 14
Cellular process	1.75E − 10
Protein metabolic process	2.65E − 07
Cell communication	1.98E − 06
Signal transduction	5.16E − 06
Immune system process	7.91E − 06
Developmental process	1.06E − 05
Transport	2.03E − 05
System process	2.12E − 04
Mesoderm development	2.14E − 04
Response to stimulus	2.90E − 04
Cell cycle	3.17E − 04
Molecular function	
Catalytic activity	2.26E − 07
Binding	1.89E − 05
Transporter activity	1.52E − 03
Peptidase activity	2.07E − 03
Transmembrane transporter activity	2.26E − 03
Hydrolase activity	2.94E − 03
Nucleic acid binding	2.99E − 03
Transferase activity	3.08E − 03
Protein binding	4.36E − 03
Receptor activity	8.88E − 03

Only top-ranked functional groups are listed. [a]*P*-values are Bonferroni corrected.

Wig-1 promotes cell cycle arrest rather than apoptosis upon cellular stress

As the absence of Wig-1 caused an increase in the proapoptotic factor FAS and a decrease in the cell cycle arrest inducer 14-3-3σ, we hypothesized that Wig-1 might have a role in controlling the outcome of cellular stress. To investigate this possibility, we silenced Wig-1 in HCT116 $p53^{+/+}$ and $p53^{-/-}$ cells and analyzed the effect on both cell cycle distribution and cell death by fluorescence activated cell sorting. We used cisplatin as a stress-inducing agent, as it induced G2 cell cycle arrest but no cell death. Upon cisplatin-induced stress, Wig-1 silencing led to a decrease in the G2 fraction of HCT116 $p53^{+/+}$ (14%) and HCT116 $p53^{-/-}$ (15%) (*P*-value = 0.001) cells relative to the control-treated cells (Figure 2a). Moreover, Wig-1 knockdown resulted in a significant increase in the sub-G1 population in both HCT116 $p53^{+/+}$ and $p53^{-/-}$ cells (Figure 2b).

Annexin V staining confirmed that the cell death induced by Wig-1 depletion upon cisplatin stress was apoptosis (Figure 2c). Thus, these results demonstrate that lack of Wig-1 leads to decreased cell cycle arrest and increased apoptosis in cisplatin-treated HCT116 $p53^{+/+}$ and $p53^{-/-}$ cells. This effect is p53-independent, as we observed similar effects in both HCT116 $p53^{+/+}$ and $p53^{-/-}$ cells.

To examine whether the observed shift of the cellular stress response toward apoptosis has any impact on cell growth and survival over longer time, we also examined the effects of Wig-1 knockdown in a long-term growth assay. We transfected HCT116 $p53^{+/+}$ and $p53^{-/-}$ cells with Wig-1 siRNA, treated the cells with cisplatin and kept the cells in culture for an additional 3 days. We assessed cell growth and viability by counting living cells using Trypan blue exclusion (Figure 2d) and Giemsa staining (Figure 2e). This revealed a significantly decreased viability after Wig-1 knockdown.

We also examined HCT116 $p53^{+/+}$ and $p53^{-/-}$ cells after treatment with another stress agent, gamma irradiation, which induces G2 arrest in both cell lines. After Wig-1 knockdown, we observed a significant decrease in G2 arrest (18%) (*P*-value = 0.04) and an increased cell death in HCT116 $p53^{+/+}$ cells. We did not observe any significant changes in cell cycle arrest or cell death in HCT116 $p53^{-/-}$ cells (Supplementary Figures 2a and b)

In parallel, we studied the effect of Wig-1 knockdown in wild-type p53-carrying U2OS cells upon induction of cellular stress. Gamma irradiation induced G2 arrest in U2OS cells, which was decreased by 13% after Wig-1 knockdown, along with increased cell death (Supplementary Figures 3a and b). In contrast, cisplatin had little effect on cell cycle distribution, and Wig-1 knockdown only induced a minor increase in the G1 and G2 fractions upon cisplatin treatment. However, Wig-1 knockdown

a

Gene	Name	Gene expression values, Log2(siW1/siC) Array 1	Array 2	Array 3	Mean	AU-rich element	Validation
FAS	Fas (TNF receptor superfamily, member 6)	4,37	4,44		4,41	Yes	Yes
WNT1	Wingless-type MMTV integration site family, member 1	4,59	3,76		4,18	No	Yes
FZD8	Frizzled homolog 8 (Drosophila)		3,13	3,72	3,43	Yes	No
AKT3	V-akt murine thymoma viral oncogene homolog 3 (protein kinase B, gamma)	2,12	3,24		2,68	Yes	Yes
APP	Amyloid beta (A4) precursor protein	2,38	2,05	3,17	2,53	Yes	Yes
SFN	Stratifin (14-3-3σ)	-4,89	-2,1		-3,50	No	Yes
CDC42	Cell division cycle 42 (GTP binding protein, 25kDa)	-2,3	-2,22		-2,42	Yes	No
PPP2CB	Protein phosphatase 2 (formerly 2A), catalytic subunit, beta isoform (PP2A)	-1,87	-2,65	-2,35	-2,29	Yes	Yes

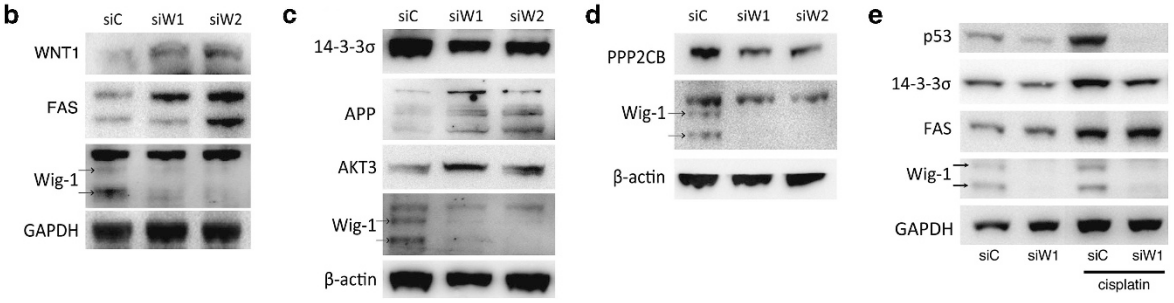

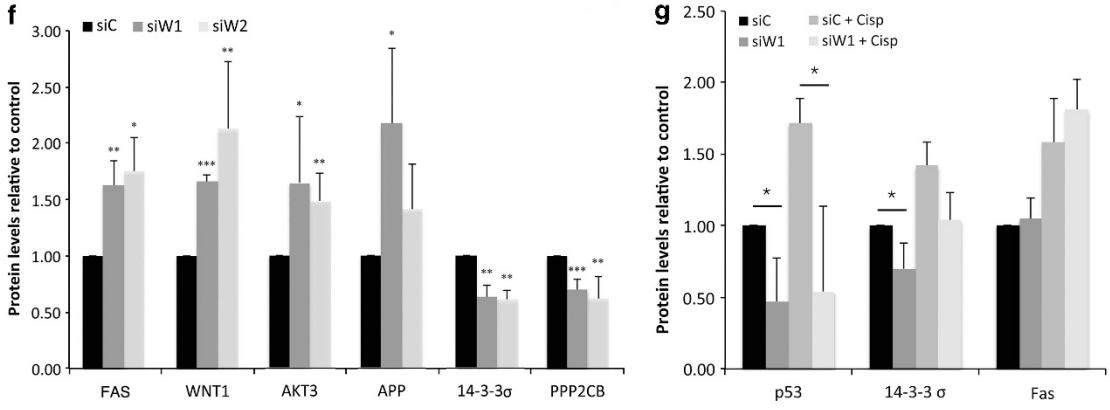

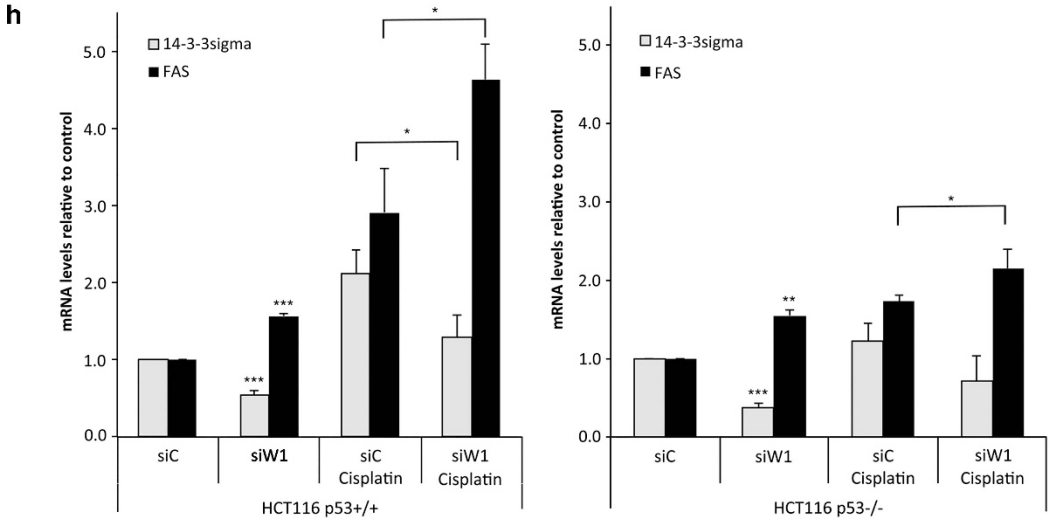

Figure 1. Microarray target validation after Wig-1 knockdown. List of targets selected for validation with their microarray gene expression levels (**a**). Wig-1 knockdown (siW1, siW2) in HCT116 p53$^{+/+}$ cells leads to increased FAS, WNT1, AKT3 and APP (**b**, **c**) and decreased 14-3-3σ and PPP2CB protein levels (**c**, **d**), confirming the microarray results. Arrows indicate the two major Wig-1 species. Protein-level quantifications are shown in (**f**). The same effect on 14-3-3σ and FAS protein levels after Wig-1 knockdown in HCT116 p53$^{+/+}$ cells is also observed after stress induction by cisplatin (5 μM for 24 h) (**e**). Protein level quantifications are shown in (**g**). Wig-1 knockdown leads to decreased levels of 14-3-3σ mRNA and increased levels of FAS mRNA in HCT116 p53$^{+/+}$ and p53$^{-/-}$ (**h**) cells in the presence and absence of cisplatin (5 μM 24 h), as assessed by qRT–PCR. The figure shows 14-3-3σ and FAS mRNA levels relative to mRNA levels in control siRNA-transfected untreated cells. Representative image from one of three independent experiments are shown in (**b**–**e**). Columns and error bars in (**f**–**h**) represent the mean ± s.d.; $n = 3$; ***$P < 0.001$; **$P < 0.01$; *$P < 0.05$.

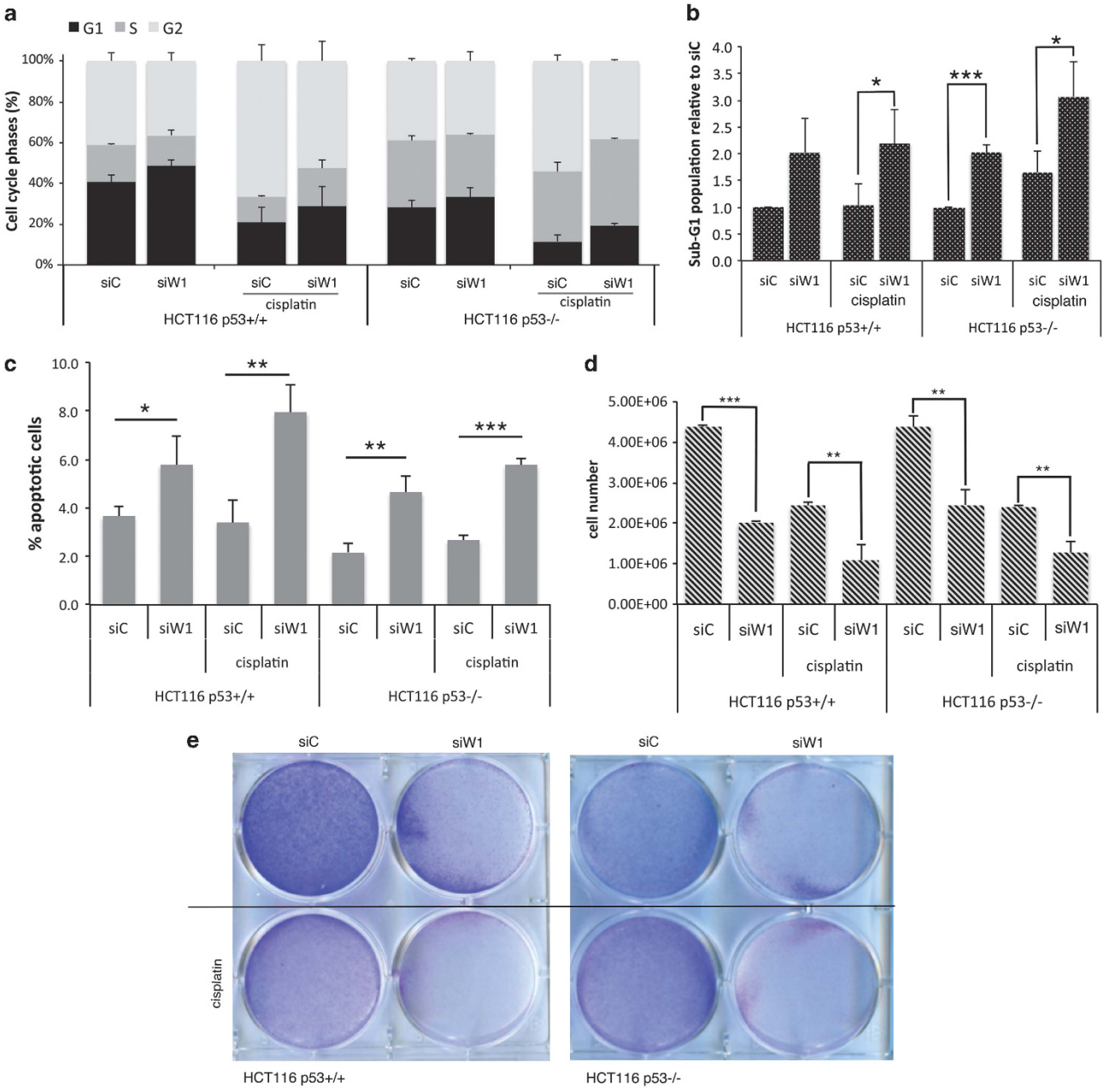

Figure 2. Wig-1 knockdown leads to cell death rather than cell cycle arrest upon cellular stress in HCT116 cells. FACS analysis of cell cycle distribution in HCT116 $p53^{+/+}$ and $p53^{-/-}$ cells transfected with control siRNA or siRNA targeting Wig-1 (siW1) demonstrates a decrease in the G2 (**a**) and an increase in the sub-G1 population (**b**) after treatment with cisplatin (5 μM 24 h). Annexin V staining confirmed that the observed cell death was due to apoptosis (**c**). Decreased proliferation/cell viability 4 days after Wig-1 knockdown and 5 μM cisplatin treatment or no treatment is shown by live cell number count using Trypan blue exclusion (**d**) and Giemsa staining of fixed cells in cell culture dishes (**e**). Columns and error bars represent the mean ± s.d.; $n = 3$; $^{***}P < 0.001$; $^{**}P < 0.01$.

resulted in a markedly increased cell death in both untreated and cisplatin-treated cells (Supplementary Figure 3b). This is consistent with the finding that FAS mRNA levels increased after Wig-1 depletion, whereas 14-3-3σ levels were unchanged (Supplementary Figure 3c).

Next, we assessed the effect of Wig-1 silencing in primary human dermal fibroblasts (HDFs) with or without gamma irradiation. Gamma irradiation (6 Gy) induced G1 and G2 arrest after 24 h in both AGO1519B and AGO1523C HDFs, as assessed by fluorescence-activated cell sorting (FACS) (sub-G1 fraction). Wig-1 knockdown led to a significant decrease of the G1 fraction in irradiated AGO1519B (12%; *P*-value = 0.002) and AGO1523C (7%; *P*-value = 0.002) cells as compared with the irradiated control-transfected cells (Figure 3a). No significant effect on the sub-G1 population was observed after Wig-1 knockdown (Figure 3b). We assessed the effect of Wig-1 knockdown in long-term assays, as described above for HCT116 cells. Wig-1 knockdown inhibited proliferation of gamma-irradiated normal fibroblasts, as shown by counting living cells and by light microscopy (Figures 3c and d). Taken together, our data demonstrate that Wig-1 promotes cell cycle arrest in normal fibroblasts upon gamma irradiation and promotes long-term cell survival. We did not detect significant cell death in these HDFs, which may reflect the fact that normal fibroblasts show increased resistance to apoptosis.[25]

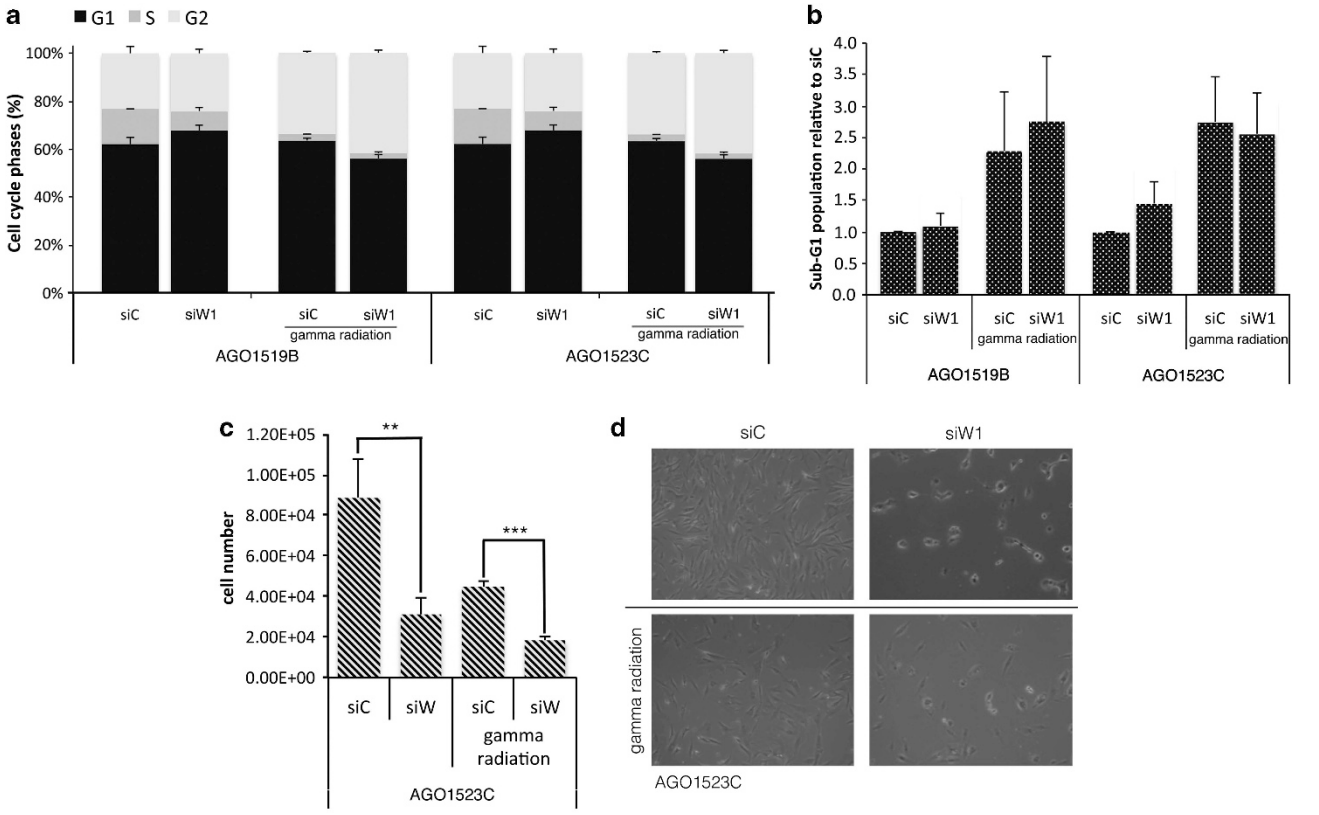

Figure 3. Wig-1 knockdown in normal fibroblasts leads to decreased survival and decreased G1 fraction upon cellular stress. FACS analysis of cell cycle distribution in HDF (AGO1519B and AGO1523C) transfected with siC or siW1 demonstrates a decrease in G1 population after gamma radiation (6 Gy, 24 h) (**a**). No increase in cell death was detected (**b**). Decreased proliferation of AGO1523C HDFs 4 days after Wig-1 knockdown and 3 days after gamma irradiation (6 Gy) is shown by live cell number count using Trypan blue exclusion (**c**) and Bright-field microscopy at $\times 100$ magnification (**d**). Columns and error bars represent the mean ± s.d.; $n = 3$; $^{**}P < 0.01$; $^{***}P < 0.01$.

Wig-1 regulates FAS mRNA at the post-transcriptional level through an ARE

To examine binding of Wig-1 to FAS mRNA, we performed RNA-immunoprecipitation assays in HCT116 and Saos-2 cells expressing Flag-tagged Wig-1, as well as Saos-2 cells expressing a mutant Wig-1 protein that lacks the first zinc-finger (Wig-1ZF1pm) and is therefore unable to bind to RNA.[13] Quantification of coimmunoprecipitated FAS mRNA revealed a four- to fivefold enrichment in immunoprecipitates of Flag-tagged wild-type Wig-1 as compared with empty vector control (Figure 4a). There was no significant enrichment of FAS mRNA in Flag-Wig-1ZF1pm immunoprecipitates (Figure 4a), indicating that zinc-finger 1 is required for Wig-1 binding to FAS mRNA.

Metabolic tagging of newly transcribed RNA by 4-thiouridine (4-sU) to investigate whether there was an effect on transcription was performed. Nascent RNA was labeled with 4-sU, extracted, conjugated to biotin and separated from pre-existing unlabeled RNA with streptavidin beads. qRT–PCR analysis of the two populations separately showed no significant variation in the 4-sU-labeled RNA, indicating no effect on FAS transcription after Wig-1 knockdown (Figure 4b). By contrast, the pre-existing, unlabeled RNA was increased by 15% upon Wig-1 silencing, suggesting an effect on mRNA stability.

Interestingly, FAS mRNA contains eight AUUUA pentamers throughout its 3′-UTR. However, only the pentamer located in the region at nucleotide position 2523–2539 (in NM_000043) is surrounded by an ARE (http://rna.tbi.univie.ac.at/cgi-bin/AREsite.cgi), which makes it the strongest putative ARE in the FAS 3′-UTR.[16] To map the regions of FAS required for Wig-1 binding, we performed *in vitro* pull-down assays using biotinylated transcripts containing the FAS 5′-UTR-ORF, FAS 3′-UTR, FAS 3′-UTR distal and FAS 3′-UTR distal dARE (constructs 1–2, 4–5; Figure 4c). The biotinylated transcripts were incubated with lysates from HCT116 $p53^{-/-}$ cells overexpressing Flag-Wig-1. After pull-down of RNA with streptavidin-coated beads, Flag-Wig-1 was readily detected by western blotting with the FAS 3′-UTR and FAS 3′-UTR distal biotinylated probe, whereas no association was found with neither FAS 5′-UTR-ORF nor FAS 3′-UTR distal dARE (Figure 4d). Thus, these results indicate that Wig-1 binds to FAS mRNA through the ARE in the distal part of the 3′-UTR.

We then performed luciferase assays to determine whether the 3′-UTR of FAS mRNA, and more precisely, the putative ARE, is responsible for Wig-1-mediated regulation. We constructed deletion mutant reporter plasmids containing different regions of FAS mRNA (Figure 4c, constructs 2–5). The 3′-UTR of p53 mRNA lacking the U-rich region (p53 3′-UTR dUs) was used as a negative control.[14] We observed a significantly increased luciferase activity upon Wig-1 knockdown with the FAS 3′-UTR and FAS distal 3′-UTR reporter plasmids but not with the other constructs (Figure 4e). Taken together, these results support the notion that Wig-1 directly targets and regulates FAS mRNA through the ARE in the distal 3′-UTR.

Wig-1 interacts with deadenylase subunit CNOT6 and FAS mRNA in stress granules

To delineate the mechanism of Wig-1-dependent regulation of FAS mRNA stability, we silenced known components of the ARE-mediated mRNA decay pathway. We knocked down the expression of CNOT6 (subunit of the CCR4–NOT deadenylation complex), PmScl-75 (exonuclease of the exosome), DCP1a (5′-decapping enzyme) and XRN1 (5′- to 3′- exoribonuclease). As shown in

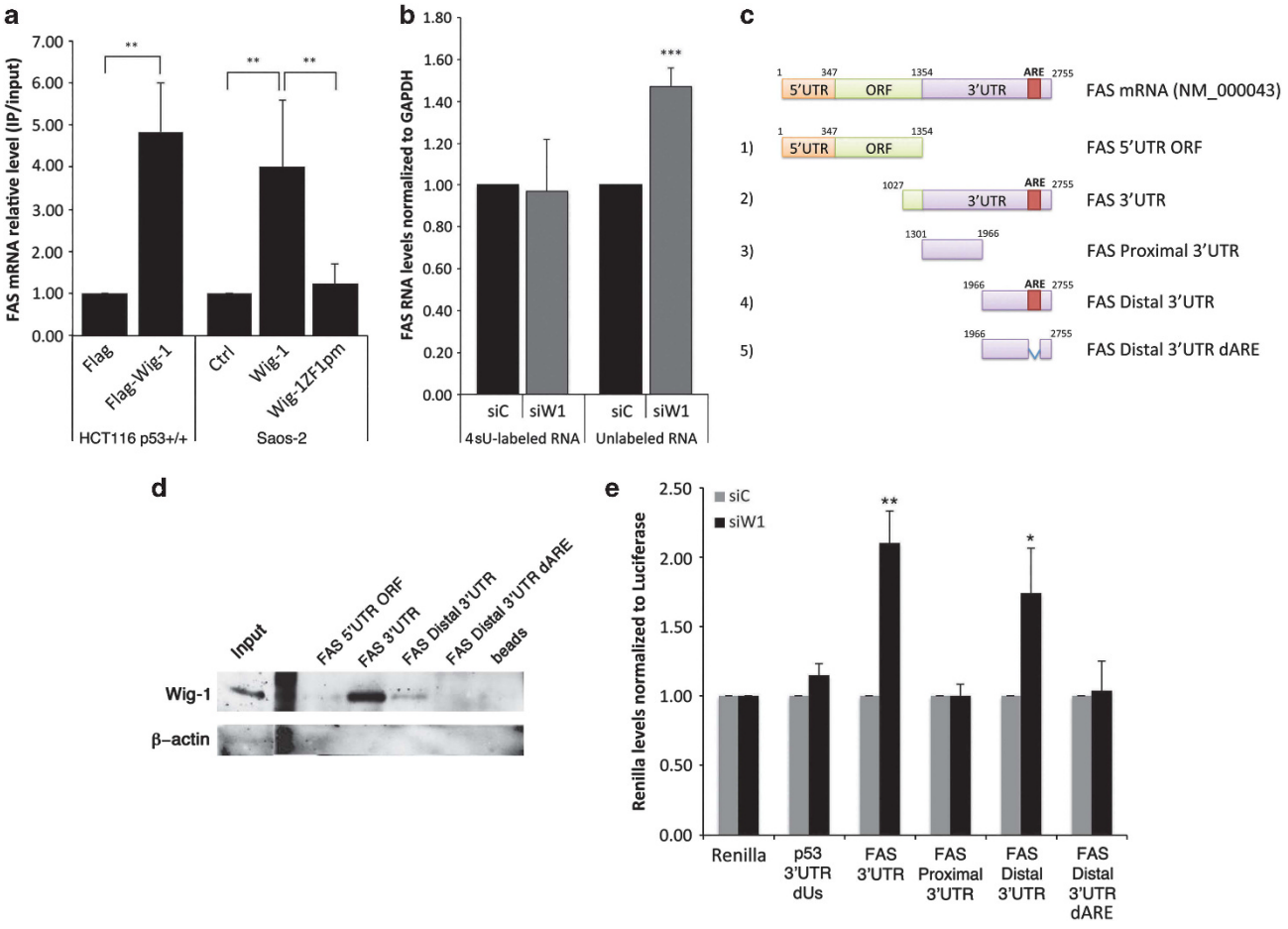

Figure 4. Wig-1 binds to the 3′-UTR of FAS mRNA and regulates its stability through the ARE. RNA immunoprecipitation was performed in HCT116 cells transiently transfected with pCMVtag2b (Flag) or pCMVtag2bhWig-1 (Flag-Wig-1) and in Saos-2 TetON cells without insert (Ctrl) or Saos-2 TetON cells stably transfected with either Flag-tagged wt Wig-1 (Wig-1) or a Flag-tagged Wig-1 zinc-finger 1 point mutant that cannot bind to RNA (Wig-1ZF1pm) (**a**). Wig-1 was precipitated with anti-Flag beads, and bound RNA was purified and quantified by qRT–PCR. GAPDH mRNA levels were used as internal control. Labeling of nascent RNA with 4-sU, RNA extraction, conjugation of the 4-sU to biotin and separation of nascent and older RNA with streptavidin beads followed by qRT–PCR analysis of the two populations separately showed no significant variation in the 4-sU-labeled RNA, whereas we observed an increase in the older, unlabeled RNA population after Wig-1 knockdown. GAPDH was used as internal control (**b**). Biotin pull-down assay using FAS 5′-UTR-ORF, FAS 3′-UTR, FAS 3′-UTR distal and FAS 3′-UTR distal dARE probes (**c**) followed by western blotting for Wig-1 shows that Wig-1 binds to the ARE in the 3′-UTR of FAS. (**d**). Representative image from one of two independent experiments. To determine whether the ARE is required for Wig-1 regulation of FAS mRNA, we generated the constructs 2–5 described in (**c**) or the p53 3′-UTR lacking the ARE as negative control and cloned them downstream of the Renilla reporter into the psiCheck-2 vector. Luciferase assays confirmed that the ARE in the 3′-UTR of FAS mRNA is essential for regulation by Wig-1, as constructs lacking this ARE do not show increased activity after Wig-1 depletion (**e**). Columns and error bars in (**a**), (**b**) and (**e**) represent the mean ± s.d.; $n = 3$; ***$P < 0.001$; **$P < 0.01$; *$P < 0.05$.

Figure 5a, Wig-1 or CNOT6 knockdown in HCT116 p53$^{-/-}$ cells led to a similar increase in FAS mRNA levels, whereas the increase of FAS mRNA after silencing of other degradation pathway enzymes was significantly lower. This result suggests that CNOT6 is responsible for degrading FAS mRNA. We propose that Wig-1 recruits the CCR4–NOT complex to FAS mRNA and thereby triggers its deadenylation, leading to inhibition of FAS expression.

To determine whether Wig-1 directly interacts with CNOT6, we performed coimmunoprecipitation experiments with exogenous Wig-1 in HCT116 p53$^{+/+}$ and p53$^{-/-}$ cells expressing Flag-tagged Wig-1. Endogenous CNOT6 protein was coimmunoprecipitated with Flag-Wig-1 (Figure 5b). This interaction was confirmed in a reverse coimmunoprecipitation with an anti-CNOT6 antibody (Figure 5b). This interaction was also confirmed in HCT116 p53$^{+/+}$ cells upon cisplatin treatment (Supplementary Figure 4).

The CCR4–NOT complex is known to regulate gene expression in response to stress.[26] To explore whether CNOT6 interacts with Wig-1 upon stress, we determined whether CNOT6 colocalizes with Wig-1 after arsenite-induced stress using coimmunostaining in HCT116 p53$^{+/+}$ cells. Under unstressed conditions, both proteins localize uniformly throughout the cytoplasm, although Wig-1 is predominantly nuclear. As the uniform cytoplasmic distribution makes colocalization studies difficult, we used arsenite, an inducer of stress granules (SGs) and processing bodies, for these experiments. The formation of these structures facilitates protein colocalization studies. We found that arsenite caused relocalization of both Wig-1 and CNOT6 to SGs, as shown by coimmunostaining with the SG marker TIAR (Figures 5c and d) but not with the processing body marker HEDLS (Supplementary Figure 5a). Arsenite-induced stress did not affect Wig-1 or p53 protein levels (Supplementary Figure 6), suggesting that the observed Wig-1 accumulation in SGs is indeed the result of cytoplasmic re-distribution. To investigate whether FAS mRNA also colocalizes with Wig-1 to SGs, U2OS cells were treated with arsenite and FAS mRNA was detected by RNA-FISH using an FAS

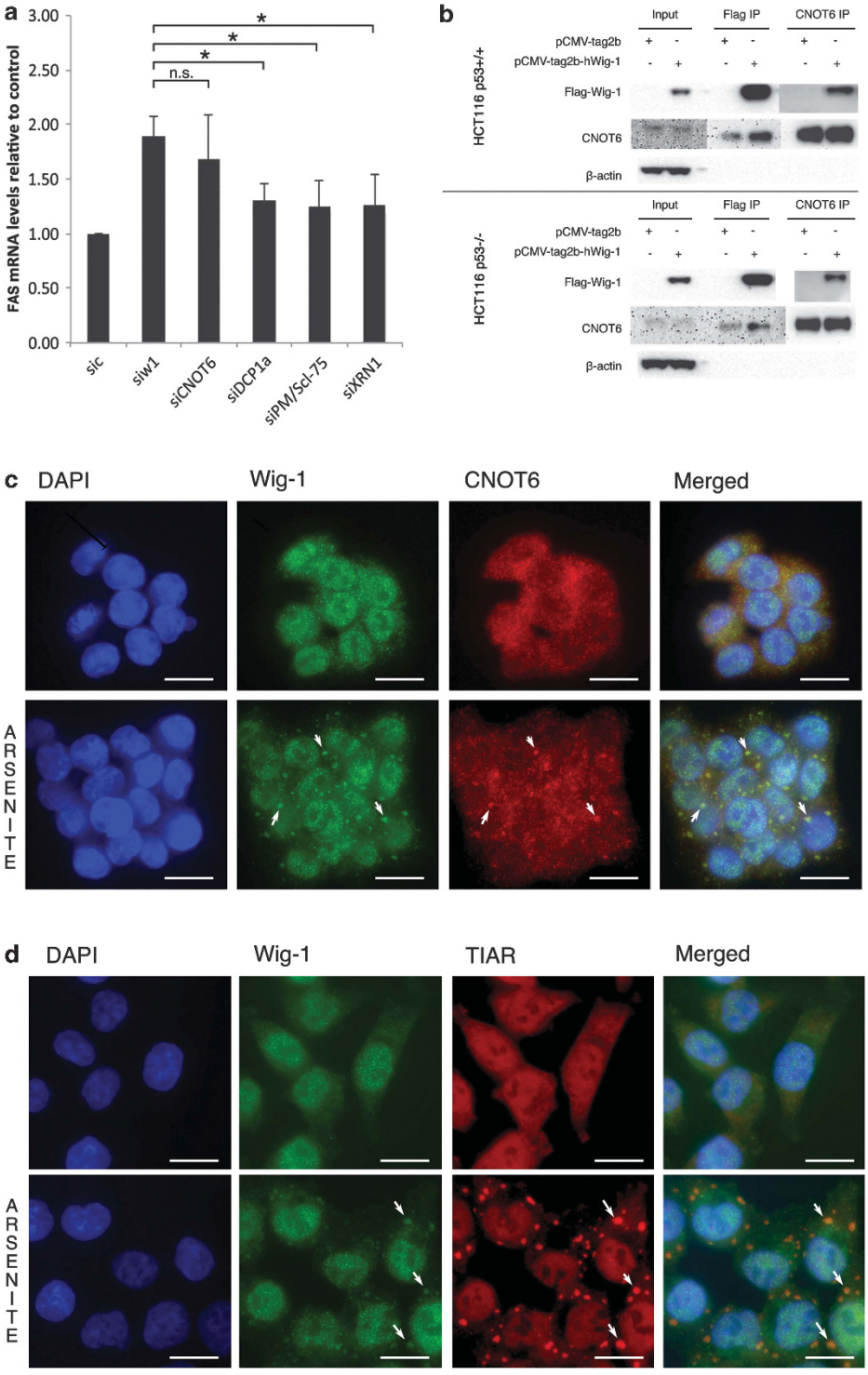

Figure 5. Wig-1 interacts with deadenylase subunit CNOT6. Knockdown of the key components of the ARE-mediated mRNA decay pathway CNOT6, DCP1a, PM/Scl-75 and XRN1 was performed in HCT116 $p53^{-/-}$ cells, and the levels of FAS mRNA were assessed through qRT–PCR and compared with levels upon Wig-1 depletion. The figure shows that FAS mRNA levels are increased in a comparable manner following knockdown of CNOT6 or Wig-1 (no significant difference), suggesting that the Wig-1 effect on FAS mRNA is exerted at the level of poly(A) tail deadenylation (**a**). Protein lysates from HCT116 $p53^{+/+}$ or HCT116 $p53^{-/-}$ cells transfected with pCMVtag2b or pCMVtag2bhWig-1 were immunoprecipitated with a Flag antibody or CNOT6 antibody cross-linked to Dynabeads Protein G, followed by western blotting with indicated antibodies (**b**). Coimmunostaining of endogenous Wig-1 (green) and CNOT6 (red) (**c**) and Wig-1 (green) and SGs marker TIAR (red) (**d**) in HCT116 $p53^{+/+}$ cells after 30 min of treatment with 0.5 mM arsenite shows colocalization in cytoplasmic SGs. Arrows indicate the positions of overlapping Wig-1 and CNOT6 foci or Wig-1 and TIAR. Scale bars, 20 μm. DAPI shows DNA staining.

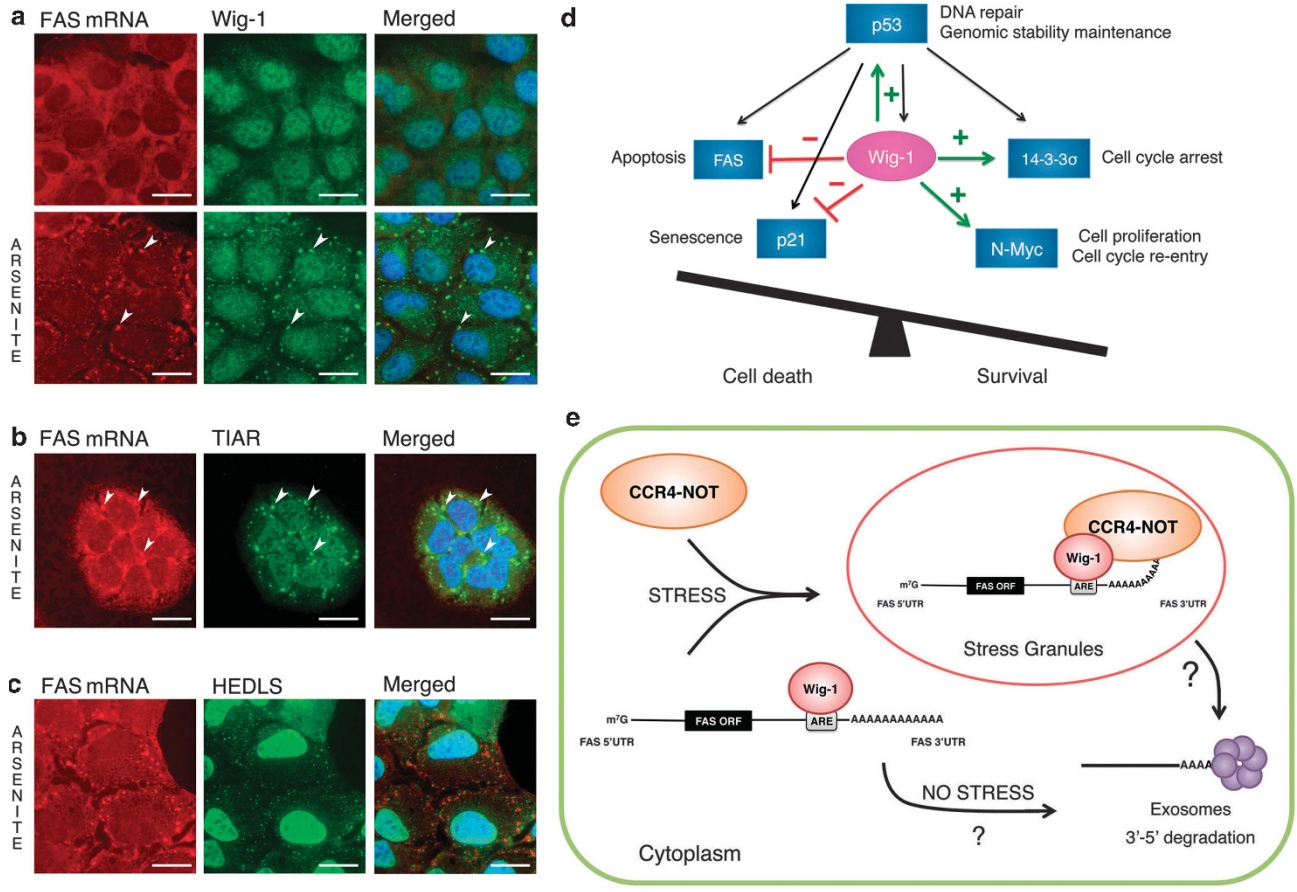

Figure 6. FAS mRNA colocalizes with Wig-1 protein in SGs. RNA FISH staining for FAS mRNA together with anti-Wig-1 (**a**), anti-TIAR (**b**) or anti-HEDLS (**c**) antibody in untreated or treated (0.5 mM arsenite) U2OS cells. TIAR and HEDLS proteins were used as SG and processing body marker, respectively. Arrows indicate the positions of overlapping FAS mRNA and Wig-1 or TIAR proteins. Scale bars, 20 μm. Blue dye shows DAPI DNA staining. Representative images from one of two independent experiments are shown. (**d**) Model for the role of Wig-1 in regulation of cell death and survival in the p53 stress response. (**e**) Model for Wig-1-mediated post-transcriptional regulation of FAS mRNA.

mRNA fluorescent probe. Coimmunostaining with antibodies against either endogenous Wig-1 (Figure 6a) or TIAR (Figure 6b) confirmed colocalization of FAS mRNA with Wig-1 in SGs. No FAS mRNA colocalized with HEDLS in the processing body.(Figure 6c; see Supplementary Figure 5b–d for additional examples and negative control data with the sense FAS probe). These results suggest that Wig-1 and CNOT6 proteins interact with FAS mRNA in cytoplasmic SGs after cellular stress.

DISCUSSION

Our microarray analysis revealed that Wig-1 silencing affects a large set of mRNAs directly or indirectly. Functional annotation of the target genes indicates the p53 pathway as one of the most affected pathways, together with Alzheimer's and Huntington's diseases, the FAS signaling pathway and apoptosis. Our data thus suggest that Wig-1 has a role in multiple cellular processes and pathways, consistent with previous studies showing that ARE-BPs, such as HuR and AUF1, regulate multiple mRNA targets. AUF1 can bind to and destabilize ARE-containing mRNAs such as c-Myc and TNF-α but has also been reported to stabilize other ARE-containing mRNAs such as cyclin D1 and c-Fos.[27–29] HuR, usually described as a stabilizer of multiple mRNAs, including cyclin A, cyclin B1 and c-Fos,[30,31] has been shown to destabilize the mRNAs of p16[32] and c-Myc.[33]

As Wig-1 is a direct p53 target and a regulator of p53 mRNA,[14] we were not surprised to find the p53 pathway and the apoptosis pathway among the pathways that were significantly affected in the absence of Wig-1. The evidence indicating that Wig-1 has an impact on diseases of the nervous system is in accordance with the fact that Wig-1 is expressed at high levels in the brain,[10] as well as with the involvement of the Wig-1 rat homolog, PAG608, in ischemia and oxidative stress-induced apoptosis in the nervous system.[34,35] Moreover, a recent study in mice indicated that Wig-1 is involved in neurodegenerative diseases such as Huntington's disease.[36]

We found that Wig-1 silencing leads to increased levels of the proapoptotic factor FAS and reduced levels of the cell cycle arrest-associated factor 14-3-3σ, suggesting that Wig-1 can modulate the cellular stress response such that cell cycle arrest is favored over apoptosis. Indeed, we show that Wig-1 silencing enhanced apoptosis and reduced cell cycle arrest in response to cellular stress in HCT116 cells. Importantly, our data demonstrate that Wig-1 can regulate FAS and 14-3-3σ independently of p53, as evidenced by the similar effect in both p53 wild-type and null HCT116 cells with and without cisplatin-induced stress. We therefore propose that Wig-1 acts to maintain high levels of 14-3-3σ (thus promoting cell cycle arrest) while at the same time repressing FAS (and thus, repressing apoptosis), the net outcome being increased survival. After mild stress, Wig-1 levels are further increased by p53, suggesting that p53 uses Wig-1 as an effector to tip the cellular response toward survival. In HCT116 $p53^{-/-}$ cells, Wig-1 is not induced in response to stress. Nonetheless, inhibition of basal Wig-1 expression by knockdown in these cells has a negative effect on cell survival, demonstrating that Wig-1 acts as a survival factor also in p53 null cells (Figure 6d). This prosurvival

role of Wig-1 is not confined to cancer cell lines. Silencing of Wig-1 also leads to decreased long-term survival in HDF cells. This effect was not associated with increased apoptosis, presumably because of a general apoptosis resistance in normal human fibroblasts.[25] Instead, a recent report indicated that Wig-1 knockdown can induce senescence in fibroblasts by regulating p21 levels.[37]

We show that the proapoptotic p53 target FAS is a direct Wig-1 target at the mRNA level. We found that Wig-1 binds to the ARE in the 3′-UTR of FAS mRNA and that the binding is mediated by the first zinc-finger in Wig-1. Moreover, the ARE is responsible for Wig-1-mediated regulation of FAS mRNA. Removal of the 17 nucleotides composing the ARE completely abrogates binding and regulation. We observed weaker binding to the FAS 3′-UTR distal RNA (Figure 4d). A reason for the weaker binding to the FAS 3′-UTR distal RNA compared with the full-length FAS 3′-UTR could be that the short 3′-UTR distal RNA may not entirely recapitulate the local secondary structure of the full-length FAS mRNA in the region around the ARE, which will therefore bind less efficiently to Wig-1.

We found that Wig-1 colocalizes and interacts with a component of the deadenylase complex CCR4–NOT, CNOT6,[26,38] suggesting that Wig-1 may mediate the interaction between the complex and FAS mRNA, thus enhancing FAS mRNA degradation. This idea is supported by our finding that Wig-1 or CNOT6 knockdown results in similar increases in FAS mRNA levels. Thus, we conclude that FAS mRNA regulation is associated with altered deadenylation rate mediated by the CCR4–NOT complex. This is particularly interesting, as it suggests a molecular mechanism for Wig-1-mediated ARE-dependent regulation.

Immunofluorescence staining and RNA-FISH revealed that the Wig-1, CNOT6 and FAS mRNA all localize in SGs upon arsenite stress. Untranslated mRNAs and proteins that regulate mRNA turnover accumulate within SGs as a consequence of stress-induced translational arrest. Transcripts in SGs are subjected to mRNA triage and are re-routed to sites of translation reinitiation, storage or degradation.[39] For example, the ARE-binding protein TTP localizes to SGs after arsenite stress, causing its associated mRNAs to undergo translational arrest. TTP promotes mRNA decay by recruiting components of the mRNA degradation machinery, including components of the CCR4–NOT complex Not1 and Caf1, to ARE-containing transcripts in the cytoplasm.[40] We suggest that under stress conditions, in which translation is repressed and SGs are formed, the colocalization of Wig-1, CNOT6 and FAS mRNA stimulates the interaction between these three factors, causing enhanced FAS mRNA degradation in the SGs and/or relocalization of FAS to other specialized mRNA degradation sites. Under normal conditions, Wig-1 binds FAS mRNA through recognition of its ARE in the cytoplasm and promotes its degradation in a similar manner, but presumably with lower efficiency (Figure 6e).

The findings presented here provide a significantly improved understanding of the biological function of Wig-1 protein. We demonstrate a novel mechanism of direct regulation of FAS mRNA at the post-transcriptional level, where Wig-1 binds to the ARE in the FAS 3′-UTR and interacts with the CNOT6 deadenylase. FAS mRNA is the first validated Wig-1 target that is destabilized in an ARE-dependent manner, in contrast to Wig-1-mediated stabilization of p53 and N-Myc mRNAs.

Our results demonstrate that Wig-1 acts as a survival factor in the p53 pathway (Figure 6d). Cellular stress triggers p53 accumulation and transactivation of p53 target genes such as 14-3-3σ, FAS and Wig-1. Levels of 14-3-3σ mRNA are further induced by Wig-1, directly or indirectly, promoting cell cycle arrest, whereas FAS mRNA is downregulated by Wig-1 through decreased mRNA stability, inhibiting cell death. This raises the question as to how the prosurvival activity of Wig-1 is regulated. It is conceivable that post-translational modifications such as phosphorylation and/or acetylation control the localization or functional activity of Wig-1 in the cell.

Taken together, we propose an important role of Wig-1 for overall cell survival. Wig-1 positively regulates N-Myc,[15] a potent driver of cell growth and proliferation. Here we show that Wig-1 favors cell cycle arrest upon activation of p53. A recent study showed that Wig-1 prevents senescence by negatively regulating the p53 target p21 at the mRNA level.[37] A prosurvival function of Wig-1 is also supported by our observation that Wig-1 null mouse embryos die before the blastocyst stage (unpublished results). We envision a scenario in which low or moderate levels of cellular stress induce p53, followed by induction of Wig-1. Wig-1 shifts the p53 response toward arrest rather than death, allowing DNA repair. Concomitant Wig-1-mediated upregulation of growth-promoting genes such as N-Myc will enable the cell to resume cell cycle progression after damage repair. In addition, Wig-1-mediated stabilization of p53 mRNA may prime the cell for a rapid p53 response to persistent stress (Figure 6d). The concept of enhanced cell survival via Wig-1-dependent mRNA regulation also raises interesting possibilities for novel cancer therapy by selective pharmacological targeting of Wig-1 in cancer cells.

In conclusion, this study indicates that Wig-1 acts as a prosurvival factor both downstream of p53 in response to moderate stress and independently of p53. Furthermore, our data demonstrate that the ARE-BP Wig-1 can regulate mRNA targets negatively, as well as positively, through binding to their AREs. Interestingly, we also demonstrate that the putative ARE in the FAS 3′-UTR is indeed functional in regulating the stability of FAS mRNA. We also suggest a mechanism through which Wig-1 can repress its target by recruiting the deadenylase machinery through interaction with the protein CNOT6.

MATERIAL AND METHODS

Cell culture, drug treatment and irradiation

HCT116 $p53^{+/+}$, HCT116 $p53^{-/-}$ and U2OS cells were grown in IMDM supplemented with 10% fetal bovine serum (GIBCO, Grand Island, NY, USA) or fetal bovine serum with reduced tetracycline (Clontech, Mountain View, CA, USA) for the tetracycline-regulated Wig-1 expressing Saos-2 cells,[13] 1% L-glutamine and 2.5 μg/ml Plasmocin (InvivoGen, San Diego, CA, USA) in 5% CO2 at 37 °C. Early-passage (population doubling <30) HDFderived from normal human neonatal foreskin (AGO1519B and AGO1523C) (Coriell Institute for Medical Research, Camden, NJ, USA) were grown in Dulbecco's modified Eagle's medium (supplemented as above). Cells were treated with 5 μM cisplatin for 24 h or exposed to 6 Gy ionizing radiation and harvested 24 h after radiation treatment. For induction of SG formation, cells were treated with 0.5 mM arsenite (Sigma, St Louis, MO, USA) for 30 min.

Cell transfection

Cell were transfected with 10 nM siRNA using HiPerFect (Qiagen, Germantown, MD, USA) according to the manufacturer's protocol. Transient plasmid transfections were performed using PEI reagent or Lipofectamine-2000 (Invitrogen, Carlsbad, CA, USA) according to the standard protocol.

Western blotting and coimmunoprecipitation

For details on buffers, see Supplementary Information, Supplementary Table 3. Preparation of total lysates and western blot analysis were carried out as described in Vilborg *et al*.[14] List of antibodies can be found in Supplementary Information. For coimmunoprecipitation, cells were lysed in VS buffer with rotation for 15 min at 4 °C. Lysates were centrifuged for 10 min at 12 000 r.p.m. and precleared for 2 h with 15 μl of Dynabeads Protein G (Life Technology, Paisley, UK). Primary antibodies were cross-linked to 15 μl of Dynabeads Protein G with dimethyl pimelimidate (Sigma) according to the manufacturer's protocol. Cross-linked beads and precleared lysate were incubated at 4 °C for 4 h under rotation, and the immunoprecipitated proteins were subjected to western blotting analysis as described above.

RNA immunoprecipitation and biotin pull-down assay

HCT116 or Saos-2 cells were harvested 24 h after transfection or 48 h after induction with 1 μg/ml doxycycline, respectively. RNA-IP was performed as

described in Vilborg *et al.*[14] For biotin pull-down assays, the pCRII-FAS-5′-UTR-ORF, pCRII-FAS-ORF-3′-UTR, pCMV6AC-FAS-distal-3′-UTR, and pCS2(+)-FAS-distal-dARE vectors were linearized with Not1 or XhoI and used as templates for *in vitro* transcription using T7 or Sp6 polymerase (Roche, Indianapolis, IN, USA) in the presence of biotin-labeling mix containing biotinylated UTPs (Roche) according to the manufacturer's protocol. 10 nM probes were then incubated with approximately 200 μg of cell lysate of HCT116 p53$^{-/-}$ cells transiently transfected with pCMVtag2bhWig-1 and used for the pull-down as described.[14]

Metabolic tagging and purification of nascent RNA

Labeling of nascent RNA with 4-sU and purification was performed as described.[41] Up to 10 μg of biotinylated RNA was isolated using Streptavidin magnetic beads (NEB, Ipswich, CA, USA) according to the manufacturer's protocol. The collected labeled and unlabeled RNA was subjected to analysis by qRT–PCR.

FACS analysis, Annexin V–FITC/PI double staining and Giemsa staining

FACS analysis was performed as described.[15] Cells were placed in six-well plates, transfected with siRNA 24 h post plating and treated with cisplatin or gamma irradiation 24 h after transfection. For apoptosis analysis, cells were plated and treated as described above, washed and resuspended in 1 × Annexin V binding buffer (BD Pharmingen, San Diego, CA, USA) and then incubated with PI and/or Annexin V-FITC in the dark for 15 min. Samples were analyzed by FACS LSRII (BD Biosciences, San Jose, CA, USA). Data were analyzed with FCS Express 4 Flow cytometry (*De Novo* software). For Giemsa staining, cells were cultured 4 days post transfection, fixed and stained with Giemsa (Sigma) according to the manufacturer's protocol.

cDNA synthesis and qRT–PCR

cDNA was synthesized using the SuperScript VILO cDNA synthesis kit (Invitrogen) or SuperScript II Reverse Transcriptase (Invitrogen) according to the manufacturer's protocol. The gene expression levels of Wig-1, FAS, 14-3-3σ and GAPDH were quantified on a 7500 Real-Time PCR System sequence detection system version 1.2 (Applied Biosystems, Foster City, CA, USA). Gene-specific probes (Applied Biosystems) were as follows: Wig-1 (Hs00536976_m1), 14-3-3σ (Hs00968567_s1), FAS (Hs00531110_m1) and GAPDH (Hs99999905_m1). The qRT–PCR was performed according to the manufacturer's recommendations. Relative gene expression was calculated by the $2^{-\Delta\Delta Ct}$ method after normalization to GAPDH levels.

Luciferase reporter assay

HCT116 p53$^{-/-}$ cells were siRNA transfected 24 h after plating, incubated for another 24 h and were subsequently transfected with either 100 ng of construct reporter vector or empty psiCheck-2 plasmid (Promega, Madison, WI, USA) for the 3′-UTR reporter assay or 100 ng of Firefly luciferase reporter plasmid or empty control plasmid co-transfected with 1 ng of Renilla control plasmid for the promoter assay. Forty-eight hours after siRNA treatment, the luciferase activity was measured using dual-luciferase reporter assay (Promega), according to the manufacturer's recommendations. The samples were read with a Wallac Victor 1420 multilabel counter (Perkin Elmer, Waltham, MA, USA). Reporter luciferase activity was normalized to control activity (Renilla to firefly activity for the 3′-UTR reporter assay, vice versa for the promoter assay).

Immunofluorescence and RNA-FISH

Following fixation and permeabilization (20 min in 4% paraformaldehyde at RT, followed by 15 min immersion in MeOH −20 °C), fixed cells were incubated with primary antibodies diluted in blocking buffer for 18 h at 4 °C. After washing with phosphate-buffered saline, cells were incubated with secondary antibodies conjugated with Alexa Fluor dye for 1 h at RT, washed in phosphate-buffered saline and mounted using HardSet mounting medium with DAPI (Vector Laboratories, Burlingame, CA, USA). RNA-FISH was performed as described.[42] FAS sense and antisense fluorescent RNA probes were generated using the FISH tag RNA red kit with Alexa Fluor 594 (Invitrogen) and the primers FAS-forward-sense (5′-ATTTAGGTGACACTATAGAAGATCCTACCTCTGGTTCTTACGTCTG-3′) or FAS-reverse-antisense (5′-TAATACGACTCACTATAGGGAGTTAGATCTGGATC-CTTCCTCTTT -3′), respectively. Images were collected using an Axioplan II imaging (Carl Zeiss, Jena, Germany) microscope equipped with a 63/1.40 immersion objective (Plan-Apochromat, Carl Zeiss).

Microarray sample preparation, hybridization and washing

Thirty micrograms of total RNA from HCT116 cells was used for the microarray analysis. Detailed methods for HEEBO oligonucleotide microarrays (by Stanford Functional Genomic Facility) are available at the Brown lab website (http://cmgm.stanford.edu/pbrown/protocols/index.html).

Microarray scanning, data filtering and analysis

Microarrays were scanned using GenePix Professional 4200A (Axon Instruments, Foster City, CA, USA), and data were collected using GenePix Pro 6.0 (Molecular Devices, Sunnyvale, CA, USA). Arrays were normalized computationally by the Stanford Microarray Database.[43] The data were filtered for signal over background of >1.5 and included for further analysis. A second filtering was done on the basis of data values including only genes whose Log(base2) of R/G Normalized Ratio (Mean) is >2 for at least two of the three arrays. Data were retrieved and exported into Microsoft excel.

Gene ontology and pathway analysis

The filtered data set was imported into PANTHER,[44] and the number of genes in each functional classification category was compared against the number of genes from the NCBI human genome in that category. The binomial test was used to statistically determine over-representation of PANTHER classification categories.[45] Bonferroni-corrected *P*-values <0.05 were considered significant.

Accession numbers

The microarray data were deposited in the GEO database under accession number GSE43046.

Statistical analysis

Student's two-tailed *t*-tests were used to determine statistical significance.

CONFLICT OF INTEREST

KGW is cofounder, shareholder and board member of Aprea AB, a company that develops p53-based cancer therapy.

ACKNOWLEDGEMENTS

We thank Stefano Caramuta for assistance with the microarray analysis and Dr Bert Vogelstein for HCT116 cells. This work was supported by grants from the Swedish Cancer Society, the Swedish Research Council (VR), the Gustaf V Jubilee Fund and a Karolinska Institutet Distinguished Professor award to KGW.

REFERENCES

1 Vousden KH, Prives C. Blinded by the light: the growing complexity of p53. *Cell* 2009; **137**: 413–431.
2 el-Deiry WS, Tokino T, Velculescu VE, Levy DB, Parsons R, Trent JM *et al.* WAF1, a potential mediator of p53 tumor suppression. *Cell* 1993; **75**: 817–825.
3 Hermeking H, Lengauer C, Polyak K, He TC, Zhang L, Thiagalingam S *et al.* 14-3-3 sigma is a p53-regulated inhibitor of G2/M progression. *Mol Cell* 1997; **1**: 3–11.
4 Muller M, Wilder S, Bannasch D, Israeli D, Lehlbach K, Li-Weber M *et al.* p53 activates the CD95 (APO-1/Fas) gene in response to DNA damage by anticancer drugs. *J Exp Med* 1998; **188**: 2033–2045.
5 Nakano K, Vousden KH. PUMA, a novel proapoptotic gene, is induced by p53. *Mol Cell* 2001; **7**: 683–694.
6 Villunger A, Michalak EM, Coultas L, Mullauer F, Bock G, Ausserlechner MJ *et al.* p53- and drug-induced apoptotic responses mediated by BH3-only proteins puma and noxa. *Science* 2003; **302**: 1036–1038.
7 Chen X, Ko LJ, Jayaraman L, Prives C. p53 levels, functional domains, and DNA damage determine the extent of the apoptotic response of tumor cells. *Genes Dev* 1996; **10**: 2438–2451.
8 Kruse JP, Gu W. Modes of p53 regulation. *Cell* 2009; **137**: 609–622.
9 Vilborg A, Bersani C, Wilhelm MT, Wiman KG. The p53 target Wig-1: a regulator of mRNA stability and stem cell fate? *Cell Death Differ* 2011; **18**: 1434–1440.
10 Varmeh-Ziaie S, Okan I, Wang Y, Magnusson KP, Warthoe P, Strauss M *et al.* Wig-1, a new p53-induced gene encoding a zinc finger protein. *Oncogene* 1997; **15**: 2699–2704.
11 Hellborg F, Wiman KG. The p53-induced Wig-1 zinc finger protein is highly conserved from fish to man. *Int J Oncol* 2004; **24**: 1559–1564.

12 Mendez-Vidal C, Wilhelm MT, Hellborg F, Qian W, Wiman KG. The p53-induced mouse zinc finger protein wig-1 binds double-stranded RNA with high affinity. *Nucleic Acids Res* 2002; **30**: 1991–1996.
13 Mendez Vidal C, Prahl M, Wiman KG. The p53-induced Wig-1 protein binds double-stranded RNAs with structural characteristics of siRNAs and miRNAs. *FEBS Lett* 2006; **580**: 4401–4408.
14 Vilborg A, Glahder JA, Wilhelm MT, Bersani C, Corcoran M, Mahmoudi S *et al.* The p53 target Wig-1 regulates p53 mRNA stability through an AU-rich element. *Proc Natl Acad Sci USA* 2009; **106**: 15756–15761.
15 Vilborg A, Bersani C, Wickstrom M, Segerstrom L, Kogner P, Wiman KG. Wig-1, a novel regulator of N-Myc mRNA and N-Myc-driven tumor growth. *Cell Death Dis* 2012; **3**: e298.
16 Beisang D, Bohjanen PR. Perspectives on the ARE as it turns 25 years old. *Wiley Interdiscip Rev RNA* 2012; **3**: 719–731.
17 Khabar KS. Post-transcriptional control during chronic inflammation and cancer: a focus on AU-rich elements. *Cell Mol Life Sci* 2010; **67**: 2937–2955.
18 Barreau C, Paillard L, Osborne HB. AU-rich elements and associated factors: are there unifying principles? *Nucleic Acids Res* 2005; **33**: 7138–7150.
19 Schoenberg DR, Maquat LE. Regulation of cytoplasmic mRNA decay. *Nat Rev Genet* 2012; **13**: 246–259.
20 von Roretz C, Di Marco S, Mazroui R, Gallouzi IE. Turnover of AU-rich-containing mRNAs during stress: a matter of survival. *Wiley Interdiscip Rev RNA* 2011; **2**: 336–347.
21 Cho SJ, Zhang J, Chen X. RNPC1 modulates the RNA-binding activity of, and cooperates with, HuR to regulate p21 mRNA stability. *Nucleic Acids Res* 2010; **38**: 2256–2267.
22 Al-Haj L, Blackshear PJ, Khabar KS. Regulation of p21/CIP1/WAF-1 mediated cell-cycle arrest by RNase L and tristetraprolin, and involvement of AU-rich elements. *Nucleic Acids Res* 2012; **40**: 7739–7752.
23 McGray AJ, Gingerich T, Petrik JJ, Lamarre J. Regulation of thrombospondin-1 expression through AU-rich elements in the 3′-UTR of the mRNA. *Cell Mol Biol Lett* 2011; **16**: 55–68.
24 Ishimaru D, Zuraw L, Ramalingam S, Sengupta TK, Bandyopadhyay S, Reuben A *et al.* Mechanism of regulation of bcl-2 mRNA by nucleolin and A + U-rich element-binding factor 1 (AUF1). *J Biol Chem* 2010; **285**: 27182–27191.
25 Di Leonardo A, Linke SP, Clarkin K, Wahl GM. DNA damage triggers a prolonged p53-dependent G1 arrest and long-term induction of Cip1 in normal human fibroblasts. *Genes Dev* 1994; **8**: 2540–2551.
26 Miller JE, Reese JC. Ccr4-Not complex: the control freak of eukaryotic cells. *Crit Rev Biochem Mol Biol* 2012; **47**: 315–333.
27 Gouble A, Grazide S, Meggetto F, Mercier P, Delsol G, Morello D. A new player in oncogenesis: AUF1/hnRNPD overexpression leads to tumorigenesis in transgenic mice. *Cancer Res* 2002; **62**: 1489–1495.
28 Lu JY, Bergman N, Sadri N, Schneider RJ. Assembly of AUF1 with eIF4G-poly(A) binding protein complex suggests a translation function in AU-rich mRNA decay. *Rna* 2006; **12**: 883–893.
29 Laroia G, Cuesta R, Brewer G, Schneider RJ. Control of mRNA decay by heat shock-ubiquitin-proteasome pathway. *Science* 1999; **284**: 499–502.
30 Wang W, Caldwell MC, Lin S, Furneaux H, Gorospe M. HuR regulates cyclin A and cyclin B1 mRNA stability during cell proliferation. *EMBO J* 2000; **19**: 2340–2350.
31 Atasoy U, Watson J, Patel D, Keene JD. ELAV protein HuA (HuR) can redistribute between nucleus and cytoplasm and is upregulated during serum stimulation and T cell activation. *J Cell Sci* 1998; **111**: 3145–3156.
32 Chang N, Yi J, Guo G, Liu X, Shang Y, Tong T *et al.* HuR uses AUF1 as a cofactor to promote p16INK4 mRNA decay. *Mol Cell Biol* 2010; **30**: 3875–3886.
33 Kim HH, Kuwano Y, Srikantan S, Lee EK, Martindale JL, Gorospe M. HuR recruits let-7/RISC to repress c-Myc expression. *Genes Dev* 2009; **23**: 1743–1748.
34 Gillardon F, Spranger M, Tiesler C, Hossmann KA. Expression of cell death-associated phospho-c-Jun and p53-activated gene 608 in hippocampal CA1 neurons following global ischemia. *Brain Res Mol Brain Res* 1999; **73**: 138–143.
35 Higashi Y, Asanuma M, Miyazaki I, Haque ME, Fujita N, Tanaka K *et al.* The p53-activated gene, PAG608, requires a zinc finger domain for nuclear localization and oxidative stress-induced apoptosis. *J Biol Chem* 2002; **277**: 42224–42232.
36 Sedaghat Y, Mazur C, Sabripour M, Hung G, Monia BP. Genomic analysis of wig-1 pathways. *PLoS One* 2012; **7**: e29429.
37 Kim BC, Lee HC, Lee JJ, Choi CM, Kim DK, Lee JC *et al.* Wig1 prevents cellular senescence by regulating p21 mRNA decay through control of RISC recruitment. *EMBO J* 2012; **31**: 4289–4303.
38 Doidge R, Mittal S, Aslam A, Winkler GS. Deadenylation of cytoplasmic mRNA by the mammalian Ccr4-Not complex. *Biochem Soc Trans* 2012; **40**: 896–901.
39 Anderson P, Kedersha N. Stress granules: the Tao of RNA triage. *Trends Biochem Sci* 2008; **33**: 141–150.
40 Sanduja S, Blanco FF, Dixon DA. The roles of TTP and BRF proteins in regulated mRNA decay. *Wiley Interdiscip Rev RNA* 2011; **2**: 42–57.
41 Dolken L, Ruzsics Z, Radle B, Friedel CC, Zimmer R, Mages J *et al.* High-resolution gene expression profiling for simultaneous kinetic parameter analysis of RNA synthesis and decay. *RNA* 2008; **14**: 1959–1972.
42 Gareau C, Fournier MJ, Filion C, Coudert L, Martel D, Labelle Y *et al.* p21(WAF1/CIP1) upregulation through the stress granule-associated protein CUGBP1 confers resistance to bortezomib-mediated apoptosis. *PLoS One* 2011; **6**: e20254, doi: 10.1371.
43 Ball CA, Awad IA, Demeter J, Gollub J, Hebert JM, Hernandez-Boussard T *et al.* The Stanford microarray database accommodates additional microarray platforms and data formats. *Nucleic Acids Res* 2005; **33**: D580–D582.
44 Thomas PD, Campbell MJ, Kejariwal A, Mi H, Karlak B, Daverman R *et al.* PANTHER: a library of protein families and subfamilies indexed by function. *Genome Res* 2003; **13**: 2129–2141.
45 Thomas PD, Kejariwal A, Guo N, Mi H, Campbell MJ, Muruganujan A *et al.* Applications for protein sequence-function evolution data: mRNA/protein expression analysis and coding SNP scoring tools. *Nucleic Acids Res* 2006; **34**: W645–W650.

Supplementary Information accompanies this paper on the Oncogene website (http://www.nature.com/onc)